Cell Metabolism
Resource

Identification of Cholesterol-Regulating Genes by Targeted RNAi Screening

Fabian Bartz,[1,2,7] Luise Kern,[1,2,7] Dorothee Erz,[1] Mingang Zhu,[2,3] Daniel Gilbert,[5] Till Meinhof,[1] Ute Wirkner,[6] Holger Erfle,[5,4] Martina Muckenthaler,[2,3] Rainer Pepperkok,[2,5,*] and Heiko Runz[1,2,*]
[1]Institute of Human Genetics
[2]Molecular Medicine Partnership Unit (MMPU), EMBL
[3]Department of Pediatrics
[4]Viroquant-Cell Networks RNAi Screening Facility, Bioquant
University of Heidelberg, Seminarstrasse 2, 69117 Heidelberg, Germany
[5]Cell Biology/Biophysics Unit, European Molecular Biological Laboratories (EMBL), Meyerhofstrasse 1, 69117 Heidelberg, Germany
[6]Department of Radiation Oncology, German Cancer Research Center (DKFZ), Im Neuenheimer Feld 280, 69120 Heidelberg, Germany
[7]These authors contributed equally to this work
*Correspondence: pepperko@embl-heidelberg.de (R.P.), heiko.runz@med.uni-heidelberg.de (H.R.)
DOI 10.1016/j.cmet.2009.05.009

SUMMARY

Elevated plasma cholesterol levels are considered responsible for excess cardiovascular morbidity and mortality. Cholesterol in plasma is tightly controlled by cholesterol within cells. Here, we developed and applied an integrative functional genomics strategy that allows systematic identification of regulators of cellular cholesterol levels. Candidate genes were identified by genome-wide gene-expression profiling of sterol-depleted cells and systematic literature queries. The role of these genes in cholesterol regulation was then tested by targeted siRNA knockdown experiments quantifying cellular cholesterol levels and the efficiency of low-density lipoprotein (LDL) uptake. With this strategy, 20 genes were identified as functional regulators of cellular cholesterol homeostasis. Of these, we describe *TMEM97* as SREBP target gene that under sterol-depleted conditions localizes to endo-/lysosomal compartments and binds to LDL cholesterol transport-regulating protein Niemann-Pick C1 (NPC1). Taken together, TMEM97 and other factors described here are promising to yield further insights into how cells control cholesterol levels.

INTRODUCTION

Elevated plasma cholesterol levels result in excess cholesterol deposition in arterial vessel walls and are a major risk factor for atherosclerosis and premature death by coronary heart disease. In the blood, cholesterol is transported as cholesterol esters in lipoprotein particles, ~70% of which are low-density lipoproteins (LDLs). For keeping blood cholesterol levels balanced, LDL cholesterol is constantly cleared by internalization into cells. The LDL receptor (LDLR) is critical in this process, as it binds and internalizes LDL via its apoB portion and clathrin-mediated endocytosis. Mutations in *LDLR* or *APOB* are a cause for the frequent genetic disorder familial hypercholesterolemia (FH) (Brown and Goldstein, 1974; Maxfield and Tabas, 2005). In the acidic environment of endocytic compartments, LDLR is released from its ligand and recycled to the cell surface, while the LDL particle is degraded in lysosomes. LDL-derived cholesterol esters are hydrolyzed, and free cholesterol is delivered to downstream organelles such as the plasma membrane, endoplasmic reticulum (ER), recycling endosomes, or mitochondria (Chang et al., 2006; Ikonen, 2008).

In the plasma membrane, cholesterol may contribute to up to 25% of membrane lipids, and it is also enriched in endo-/lysosomal compartments and the Golgi. In contrast, ER membranes are low in cholesterol. Nevertheless, being the site of cholesterol biosynthesis and the sterol-homeostatic machinery, the ER is crucial for keeping cellular sterols balanced (Goldstein et al., 2006). E.g., ER membranes retain the sterol response element-binding protein (SREBP) transcription factors in an inactive state. Once cellular cholesterol is low, SREBPs are exported from the ER to the Golgi, where they are activated by Golgi-resident proteases. The transcriptional active form of SREBP subsequently translocates into the nucleus and activates the expression of genes responsible for increasing cellular cholesterol and fatty acids. All genes known to be necessary for cholesterol biosynthesis have been suggested as putative SREBP target genes (Horton et al., 2003). Moreover, SREBPs activate genes such as *LDLR* that mediate cholesterol uptake from extracellular supplies, as well as other genes important for cellular lipid homeostasis.

Despite extensive insight into how cellular cholesterol metabolism is regulated, important questions remain: the molecular details of central transport events, e.g., how LDL-derived cholesterol leaves the lysosomes, have not yet been resolved. Little is known about the molecular interactions of the already identified cholesterol-regulating factors. And the interrelation between sterol-mediated gene expression control and subsequent events that direct cellular cholesterol homeostasis on a functional level is poorly understood. It is therefore suggested that only a limited number of proteins involved in cellular cholesterol regulation and associated membrane trafficking processes have been identified to date (Chang et al., 2006; Ikonen, 2008).

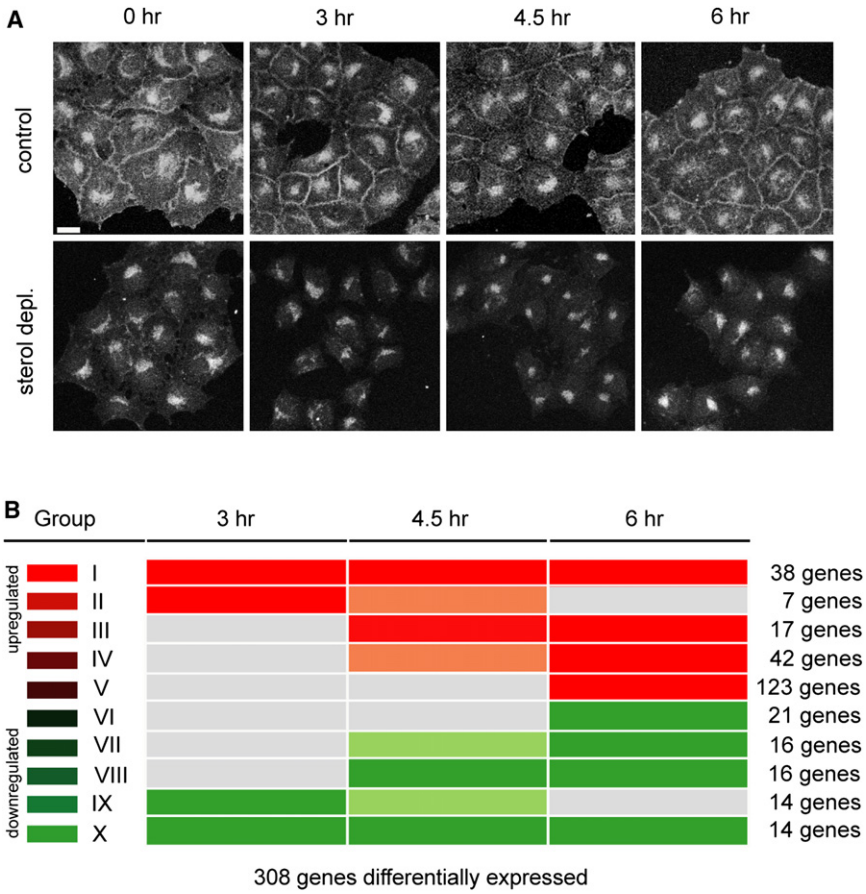

Figure 1. Gene Expression Analysis in Sterol-Depleted HeLa Cells

(A) HeLa cells were cultivated for 21 hr at 37°C, 5% CO_2 either under control (DMEM/2 mM L-glutamine/100 IU/ml penicillin/100 μg/ml streptomycin/5% FCS; medium A) or sterol-depleted (DMEM/2 mM L-glutamine/100 IU/ml penicillin/100 μg/ml streptomycin/0.5% LDS; medium B) conditions. Then, cells were fixed (0 hr) or media were exchanged for either medium A or medium B substituted with 2% (w/v) 2-hydroxypropyl-β-cyclodextrin (HPCD) for another 3 hr. Again, cells were either fixed (3 hr) or washed once with DMEM and cultivated for an additional 1.5 (4.5 hr) or 3 hr (6 hr) in medium A (controls) or medium B (sterol depl.) before staining with Filipin (50 μg/ml). Bar = 10 μm.

(B) Gene expression analysis in HeLa cells in order to identify genes with differential expression under sterol-depleted relative to control cell culture conditions. For each condition, RNAs were extracted at three different time points (3, 4.5, and 6 hr) and hybridized to human cDNA microarrays (n = 3 or 4 experiments/time point). According to magnitude and delay of transcriptional response, the 308 differentially expressed genes were classified into 10 distinct functional groups (I–X). Red/green, up-/downregulated with >2-fold; light red/light green, up-/downregulated with >1.5-fold; gray, not differentially regulated.

With the aim to identify genes with relevance to cellular cholesterol metabolism, we developed an integrative functional genomics strategy, applying genome-wide expression profiling in combination with targeted RNAi screening. For this, we established two microscope-based siRNA (small interfering RNA) screening assays that were designed to reflect (1) cellular cholesterol levels as visualized by means of cholesterol-binding dye Filipin (Börnig and Geyer, 1974) and (2) cellular internalization of fluorescence-labeled LDL (DiI-LDL) (Ghosh et al., 1994). We identified 20 genes as probably immediately relevant for maintaining cellular cholesterol levels and/or LDL uptake. Of these, we propose *TMEM97* as an SREBP target gene that in sterol-depleted cells enriches in endo-/lysosomal compartments and binds Niemann-Pick C1 (NPC1) protein, a central regulator of LDL-derived cholesterol transport out of lysosomes.

RESULTS

Genome-Wide Expression Profiling of Sterol-Depleted HeLa Cells Identifies 308 Regulated Genes

In order to identify genes with a role in cellular cholesterol metabolism, we performed genome-wide gene expression analyses in HeLa cells cultivated in lipoprotein-depleted serum (LDS) and 2-hydroxypropyl-β-cyclodextrin (HPCD) (Figure 1A). This treatment reduces cellular cholesterol levels to up to ~50% of controls and activates cellular sterol homeostatic regulatory machinery, as shown by increased levels of transcriptionally active SREBP (mSREBP) (Figure S1) (Nohturfft et al., 2000; Runz et al., 2006). Transcriptional response was monitored from sterol-depleted and control cells at three different time points by expression profiling with human cDNA microarrays (Wagner et al., 2004). In total, 308 genes showed statistically significant altered gene expression upon cellular sterol depletion. According to magnitude and delay of transcriptional response, these genes were clustered into ten different functional groups (Figure 1B; Table S1). A subset of 52 genes fulfilled the stringent criteria of being either up- or downregulated at all time points investigated. Among these, 20 genes had already previously been described as functionally relevant to cellular lipid metabolism. E.g., 16 of the 22 genes necessary for cholesterol biosynthesis in humans were represented among the genes showing strongest transcriptional activation upon sterol depletion (Table S2). Transcriptional activation of four cholesterol-synthesizing genes not represented on the microarray (*HMGCS1*, *MVD*, *LSS*, and *TM7SF2*) was independently confirmed by qRT-PCR. Expression of only two of the genes described as essential for cholesterol biosynthesis in humans (*AACS* and *PMVK*) did not respond to our sterol-depleting conditions.

Thirty-two of the fifty-two most strongly regulated genes had not previously been linked to cellular lipid metabolism. Among these, 18 genes were up- and 14 genes downregulated at all time points investigated (Table S1). Two of these genes (*SYTL2* and *SV2A*) are described as involved in membrane trafficking, three genes (*CCNG2*, *FOS*, and *TGFB2*) in cell growth/cell cycle

control, and three genes (inhibitors of DNA binding 1, 2, and 3 [*ID1*, *ID2*, and *ID3*]) in transcriptional regulation. The remaining 24 genes were either attributed to diverse functional classes or had not been further classified.

RNAi Screening Identifies 20 Genes as Functionally Relevant for Cellular Cholesterol Metabolism

We decided to analyze the functional relevance of these and other promising candidate genes by RNAi screening. To monitor the effect of candidate gene knockdown on cellular cholesterol homeostasis, two fluorescence-based assays were established for automated quantitative analysis: first, cellular cholesterol levels were measured using the cholesterol-binding dye Filipin (Börnig and Geyer, 1974; Runz et al., 2006); second, the dynamics by which DiI-LDL is internalized into cells were assayed (Ghosh et al., 1994; Gilbert et al., 2009) (Figure 2). Functional RNAi screening of multiple genes at once was achieved by using siRNA microarrays (Erfle et al., 2007), high-content screening microscopy (Liebel et al., 2003; Simpson et al., 2007), and quantitative image analysis software (Gilbert et al., 2009) (see Supplemental Data).

For systematic siRNA knockdown, we chose to target 100 preselected candidate genes (Table S3). Of these, 64 genes not previously linked to lipid metabolism were selected based on transcriptional activation or repression in response to sterol depletion (Table S1). In addition, 36 genes were chosen that had been identified as potentially relevant for cholesterol metabolism by systematic literature queries (see Experimental Procedures). Immediate functions in regulating cellular cholesterol levels and/or LDL uptake had previously been reported, to our knowledge, for only 5 of these genes (*LDLR*, *LPL*, *NPC2*, *PCSK9*, and *SCAP*). Out of these, single previously validated siRNAs against two genes, *LDLR* and Niemann-Pick C2 protein (*NPC2*) (Naureckiene et al., 2000), and the endosomal transport regulator *COPB1* (coatomer protein complex, subunit B1) (Whitney et al., 1995) were chosen as positive controls (Figures 2 and S2).

Each candidate gene was represented by six different siRNAs from two independent siRNA libraries for functional characterization with the two separate RNAi screening assays. Mean Filipin and DiI-LDL signal intensities were determined at the level of single cells in up to 15 replica arrays per siRNA library and RNAi screen (Tables S4 and S5). For each siRNA library, phenotypic effects caused by individual siRNAs were normalized to nonsilencing controls (Figure S4). Then, quantitative information of all six siRNAs per gene was averaged to a single siRNA category value per gene and RNAi screen (see Experimental Procedures). Together, both RNAi screens identified 30 genes, silencing of which resulted in cellular Filipin and/or DiI-LDL signal intensities above or below predefined cutoff thresholds, encompassing ~18% of the genes analyzed (Figures S5 and 2; Supplemental Experimental Procedures). Out of these, only those genes were considered as validated functional regulators of the respective biological process for which two or more siRNAs yielded activities larger than two SD from the mean of nonsilencing controls (deviation > 1) (Simpson et al., 2007). Excluding positive controls, 20 candidate genes fulfilled such stringent statistical criteria, validating loss of function of these genes as functionally relevant for either cellular Filipin levels or DiI-LDL uptake or both (Figure 3A, Table S6). In summary, knockdown of three candidate genes (*BHMT2*, *TMEM97*, and *VRK3*) and *LDLR* reduced both Filipin signal as well as DiI-LDL uptake. Conversely, knockdown of four candidate genes (*GBP3*, *C20orf79*, *ETV5*, and *TMSB10*) and *NPC2* increased signals in both screening assays. Interestingly, knockdown of *ID3* increased Filipin signal but reduced cellular DiI-LDL uptake, an effect similar to the knockdown of *COPB1*. Silencing of five genes (*C17orf59*, *KPNB1*, *LTBP1*, *LRP6*, and *SCAP*) reduced internalization of DiI-LDL without causing significant effects on Filipin signals. Conversely, DiI-LDL uptake was stimulated by knockdown of six genes (*AP1S2*, *FDX1*, *GOT1*, *NDRG1*, *SYTL2*, and *SYP*). Only knockdown of the gene *PSAP* increased perinuclear Filipin signal without significantly affecting DiI-LDL uptake.

LDL is internalized into cells via clathrin-mediated endocytosis, which also delivers transferrin into cells (Harding et al., 1983). Cellular uptake of transferrin depends on the transferrin receptor (*TFRC*). Knockdown of *TFRC* reliably reduces internalization of fluorescence-labeled transferrin (Tf568) into HeLa cells (Figure S6). To control the 20 genes validated as regulators in Filipin and/or DiI-LDL uptake RNAi screens for effects on transferrin uptake, we performed a third RNAi screen based on the dynamics of cellular internalization of Tf568 (Tables S4 and S5). Interestingly, knockdown of *COPB1*, *C17orf59*, and *VRK3* was validated not only to reduce cellular DiI-LDL uptake, but also to stimulate cellular internalization of Tf568 (Figures 3B and S6). Conversely, knockdown of *AP1S2* (sigma subunit of the adaptor protein 1 complex), which stimulated DiI-LDL uptake, was validated as inhibitory for Tf568 uptake. Silencing of the remaining 17 genes with functional effects on Filipin and/or DiI-LDL uptake had no significant effect on Tf568 internalization.

Comparison of Data Sets Indicates Further Genes Relevant to Cellular Cholesterol Regulation

Results from gene expression profiling and functional RNAi screening were now compared. For this, assignment to gene expression group as well as siRNA category values from Filipin and DiI-LDL uptake RNAi screens were considered for each gene (Table S7). Genes were ranked according to summarized data from all three data sets (Figure S7 and Supplemental Data). Such comparison showed not only that knockdown of *C17orf59*, *TMEM97*, and *VRK3* reduced Filipin signal and/or DiI-LDL uptake, but that these three genes were also represented among the genes with the strongest transcriptional activation in sterol-depleted cells. Conversely, *GBP3* and *ID3* mRNA levels were most strongly downregulated upon cellular sterol depletion. While knockdown of *GBP3* increased signals in both RNAi screens, silencing of *ID3* increased cellular Filipin signals but reduced DiI-LDL uptake.

Integration of gene expression results indicated further genes as of likely importance for cholesterol regulation on a functional level (Figures 3C and S7D; Movie S1). E.g., knockdown of *CYR61* by two independent siRNAs consistently reduced both Filipin signal as well as DiI-LDL uptake; nevertheless, *CYR61* was not considered as functional cholesterol regulator in RNAi screening, as the mean inhibitory effect from all six siRNAs targeting *CYR61* did not exceed predefined thresholds. However, mRNA-levels of *CYR61* were strongly downregulated in sterol-depleted cells, thus increasing the likelihood that *CYR61* is a cholesterol regulator. This was also true for further genes (see Figures 3C and S7 and Movie S1 for examples), which might turn out as

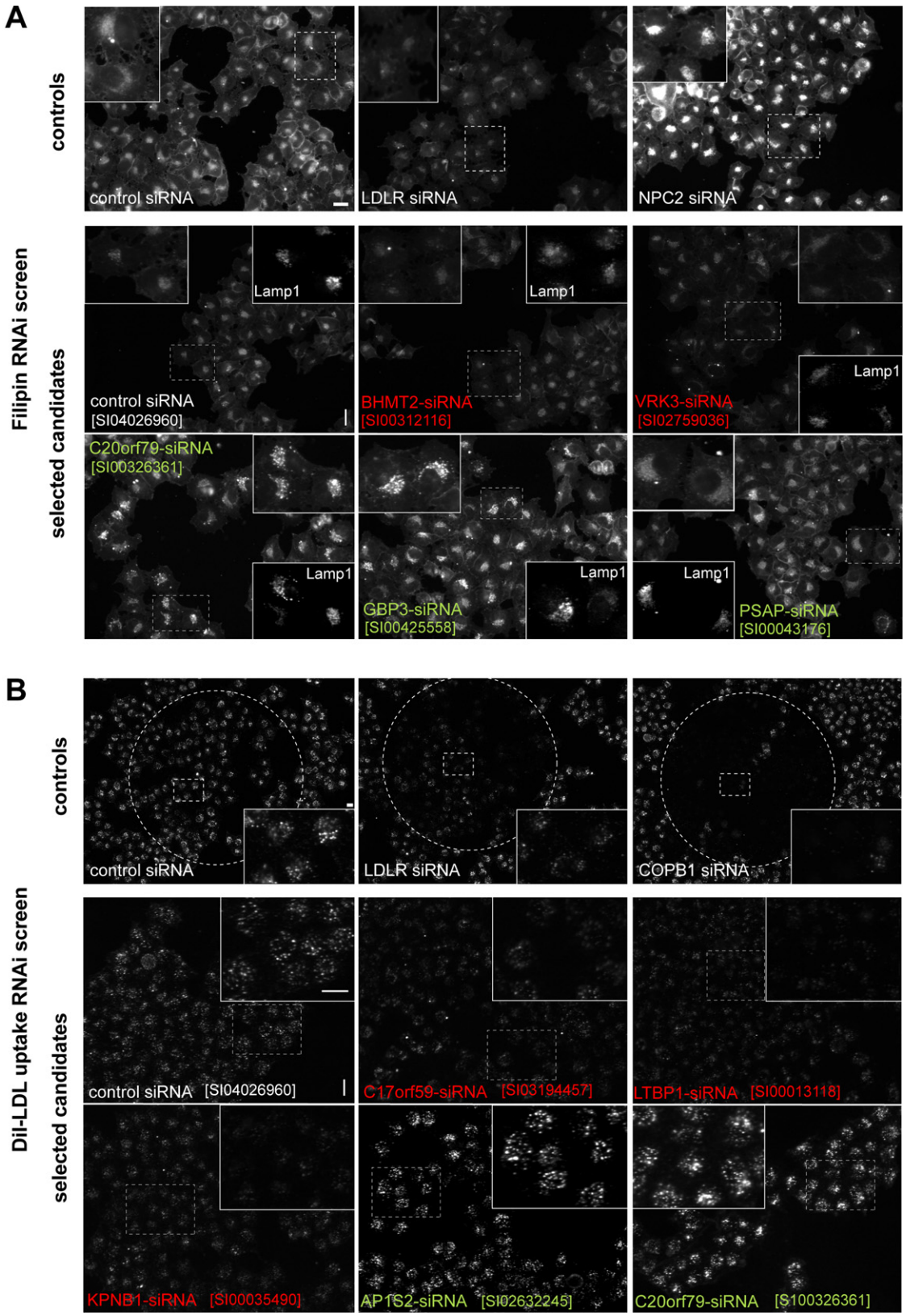

Figure 2. Filipin and DiI-LDL Uptake RNAi Screening Assays

(A and B) Functional RNAi screening for cholesterol regulating factors was performed using two cell-based assays: Filipin assay (A), in which HeLa cells cultivated under control conditions were stained with cholesterol-binding dye Filipin; and DiI-LDL uptake assay (B), in which HeLa cells cultivated in serum-free medium

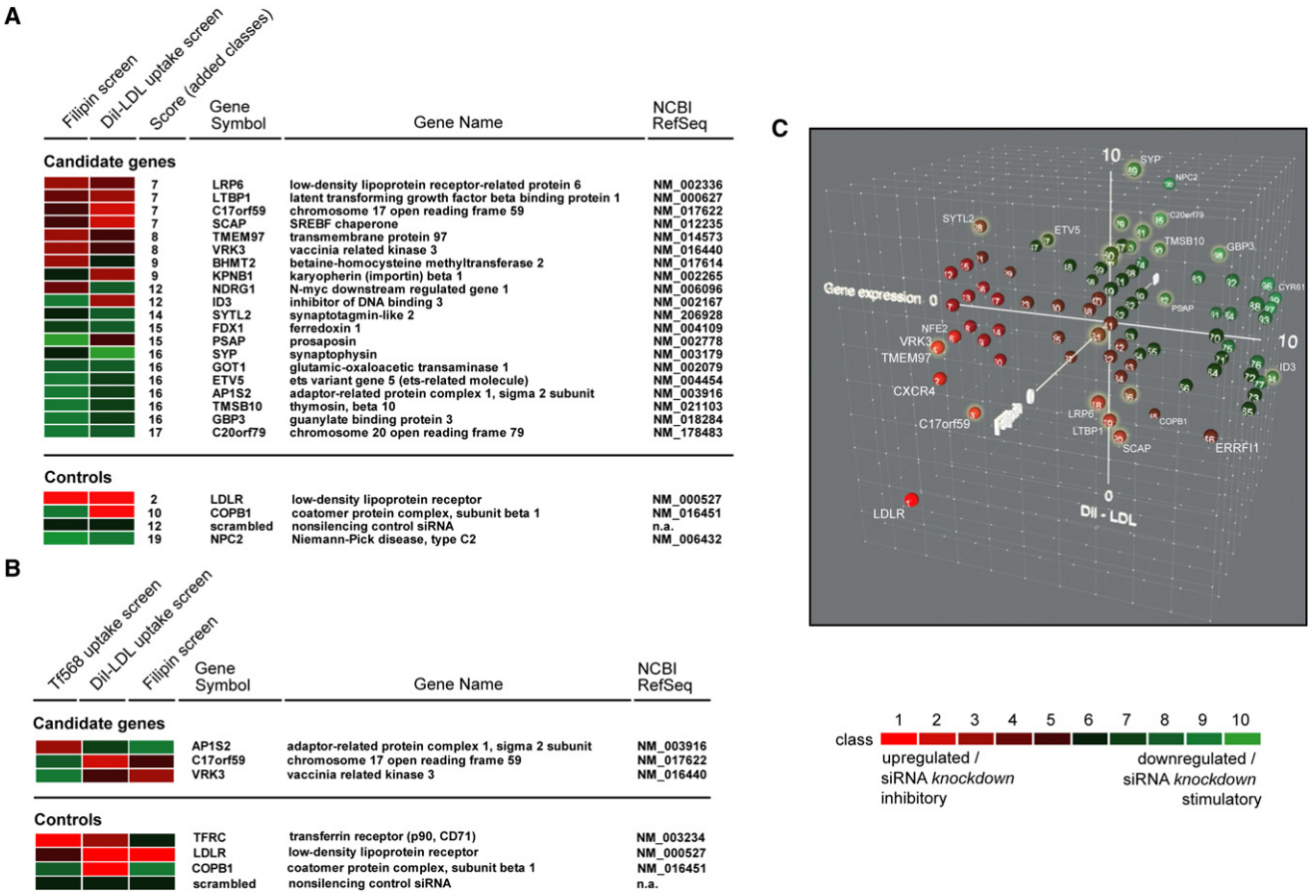

Figure 3. Genes Validated as Functional Regulators in Filipin, DiI-LDL, and Tf568 Uptake RNAi Screens

(A) Genes validated as functional inhibitors or stimulators in Filipin and/or DiI-LDL uptake RNAi screens with two or more siRNAs fulfilling requested statistical criteria (see Experimental Procedures). Genes were scored according to added class values.

(B) Genes validated as functional inhibitors or stimulators in Tf568 uptake and at least one other RNAi screen with two or more siRNAs fulfilling requested statistical criteria.

(C) Graphical representation of data from expression profiling (x axis), Filipin (y axis), and DiI-LDL uptake RNAi screens (z axis) for individual genes (colored dots) (for gene identities represented by numbers, see Figure S7D and Movie S1). Genes validated as functional regulators in RNAi screens are highlighted by coronas. Selected genes with validated or likely functional relevance to cholesterol homeostasis are highlighted by gene symbols. For animated visualization of Figure 3C, see Movie S1. Red, strongest inhibitory effect; green, strongest stimulatory effect upon siRNA knockdown.

functionally significant for cellular cholesterol regulation in follow-up studies.

TMEM97 Is a Regulator of Cellular Cholesterol Homeostasis

To test the significance of our findings, we decided to further validate one of the newly identified regulators in closer detail. We chose transmembrane protein 97 (*TMEM97*): knockdown of this gene reduced both Filipin signal as well as DiI-LDL uptake, while uptake of Tf568 was not affected (Figure 3, Tables S4–S6). Moreover, *TMEM97* mRNA levels were highly upregulated in expression profiling of sterol-depleted cells relative to controls (Table S1). With this, when data from all data sets were compared, *TMEM97* showed a ranking similar to that of *LDLR* (Figures 3C and S7, Movie S1, and Table S6).

Real-time RT-PCR confirmed that *TMEM97* mRNA levels in sterol-depleted cells were upregulated to an extent similar to those of *LDLR*; however, this upregulation was suppressed when sterols were added to the sterol-depleting culture medium (Figure 4A). Similarly, *TMEM97* expression was also strongly upregulated upon siRNA knockdown of *LDLR* (Figure 4B), which increased its mRNA levels to an extent similar to those of the cholesterol-synthesizing gene HMG-CoA reductase (*HMGCR*). Analysis of the human *TMEM97* genomic reference sequence

substituted with 0.2% (w/v) bovine serum albumin (BSA) were exposed to 1% (w/v) HPCD for 45 min and stained with 50 μg/ml DiI-LDL for 30 min at 4°C, and cellular uptake of DiI-LDL was followed for 20 min at 37.5°C before fixation. Shown are automatically acquired images of cells cultured and reverse siRNA transfected on cell microarrays for 48 hr with nonsilencing control siRNA, siRNAs known to reduce (*LDLR*) or increase (*NPC2*) cellular cholesterol levels (A) or to inhibit cellular DiI-LDL uptake (*LDLR*, *COPB1*) (B, upper panels), or siRNAs to selected candidate genes (lower panels). Red, inhibitory effect upon siRNA knockdown; green, stimulatory effect upon siRNA knockdown. Insets show magnified areas from the respective automatically acquired images. For insets from Filipin images of candidate genes, Lamp1 signal is shown.

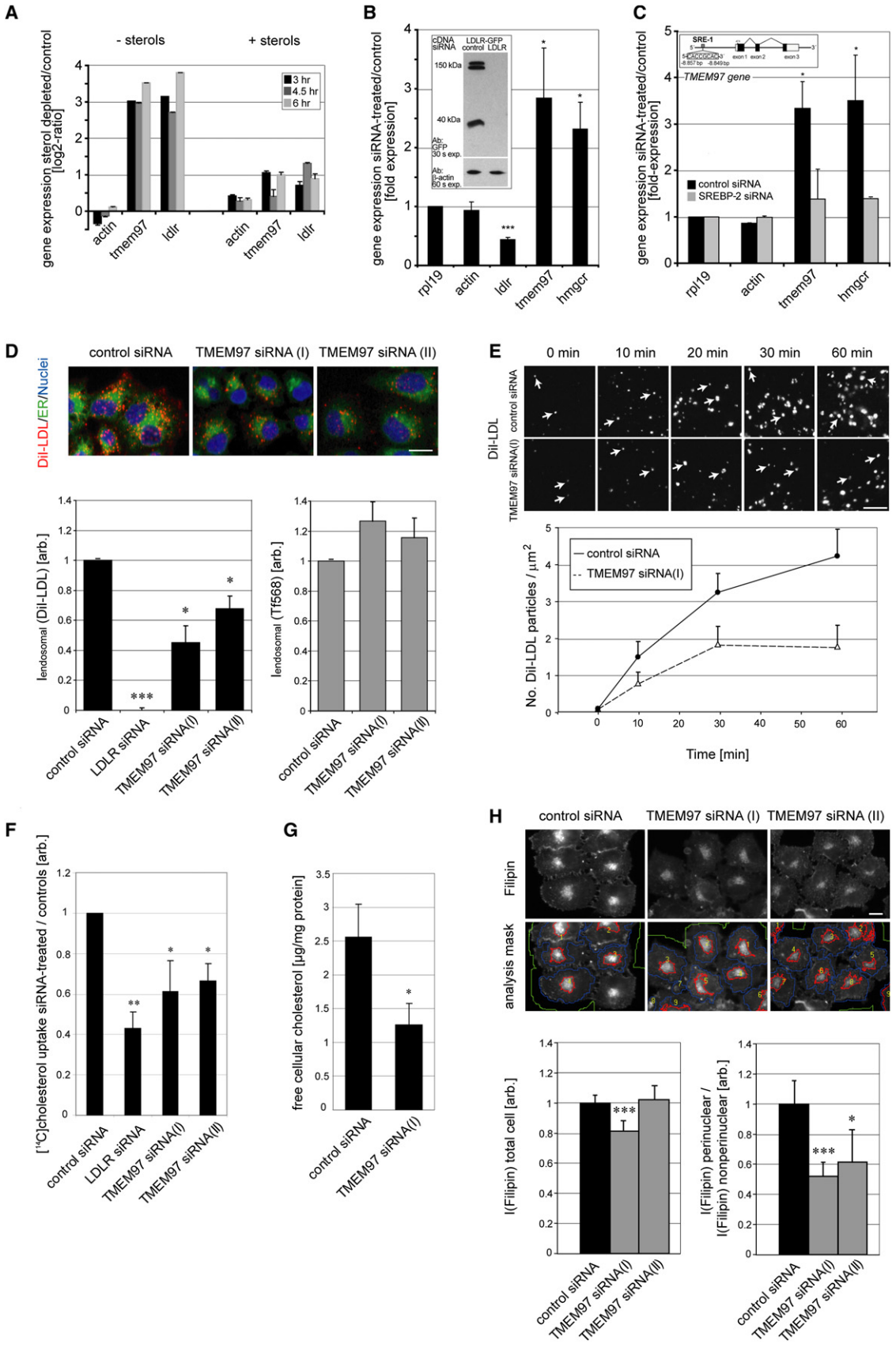
A
- sterols
+ sterols
gene expression sterol depleted/control [log2-ratio]
3 hr
4.5 hr
6 hr
actin
tmem97
ldlr
B
gene expression siRNA-treated/control [fold expression]
cDNA siRNA
LDLR-GFP control LDLR
150 kDa
40 kDa
Ab: GFP 30 s exp.
Ab: β-actin 60 s exp.
rpl19
actin
ldlr
tmem97
hmgcr
C
SRE-1
TMEM97 gene
gene expression siRNA-treated/control [fold-expression]
control siRNA
SREBP-2 siRNA
D
control siRNA
TMEM97 siRNA (I)
TMEM97 siRNA (II)
Dil-LDL/ER/Nuclei
Iendosomal (Dil-LDL) [arb.]
Iendosomal (Tf568) [arb.]
control siRNA
LDLR siRNA
TMEM97 siRNA(I)
TMEM97 siRNA(II)
E
0 min
10 min
20 min
30 min
60 min
Dil-LDL
control siRNA
TMEM97 siRNA(I)
No. Dil-LDL particles / µm2
Time [min]
F
[14C]cholesterol uptake siRNA-treated / controls [arb.]
G
free cellular cholesterol [µg/mg protein]
H
control siRNA
TMEM97 siRNA (I)
TMEM97 siRNA (II)
Filipin
analysis mask
I(Filipin) total cell [arb.]
I(Filipin) perinuclear / I(Filipin) nonperinuclear [arb.]

revealed a 5′-CACCGCAC-3′ sequence element at −8857 bp to −8849 bp upstream of the *TMEM97* transcription initiation site (Figure 4C, inset). This motif is identical to the SRE-1 consensus sequence element in the human *HMGCR* gene (Smith et al., 1990) and suggested that *TMEM97* could be an SREBP target gene. In support of this hypothesis, we observed that siRNA-mediated knockdown of *SREBP-2* suppressed transcriptional activation of *TMEM97* in sterol-depleted cells (Figure 4C).

Next, we quantified the kinetics of DiI-LDL uptake into TMEM97 knockdown cells. As anticipated from RNAi screening, targeted knockdown of TMEM97 by two distinct siRNAs to <10% of control levels (data not shown) considerably inhibited cellular DiI-LDL uptake, while cellular internalization of Tf568 was not reduced (Figure 4D). When DiI-LDL uptake into cells was followed over a time frame of 60 min, knockdown of TMEM97 reduced the number of DiI-LDL-containing endosome-like particles per cell to ~50% of controls at all time points investigated (Figure 4E). This effect could not be explained by reduced LDLR mRNA or protein levels or a reduced abundance of LDLR at the plasma membrane, which appeared unchanged under these conditions (data not shown). Similar to inhibition of DiI-LDL uptake, knockdown of TMEM97 significantly reduced cellular internalization of LDL-associated [^{14}C]cholesterol (Figure 4F). Consistent with this, total cellular levels of free cholesterol were reduced (Figure 4G). Interestingly, overall cellular Filipin signal in TMEM97 siRNA-treated HeLa cells when quantified from whole cells decreased only moderately. In contrast, when only perinuclear Filipin signal overlapping with lysosomal marker Lamp1 was quantified, Filipin intensities were more strongly reduced (Figure 4H). This effect was not due to apparent changes in lysosomal morphology or area in TMEM97 siRNA-treated cells.

TMEM97 is a conserved integral membrane protein with several sequence motifs of putative functional importance (Figures 5 and S8). To test whether TMEM97 protein may functionally compensate for reduced cholesterol levels in TMEM97 knockdown cells, we expressed epitope-tagged TMEM97 in cells in which the endogenous protein was silenced (see Supplemental Data). Coexpressing TMEM97-YFP fully rescued reduced cellular levels of free cholesterol as well as reduced Filipin signals in TMEM97 knockdown cells (Figure 5D). This confirmed that the effects observed in our knockdown experiments are indeed caused by the absence of TMEM97. Moreover, it suggested that, with respect to studying cellular cholesterol regulation, TMEM97 constructs are likely to reflect the function of the endogenous protein.

We next localized TMEM97 in living cells. Transient expression of TMEM97-YFP in HeLa cells cultivated under control conditions revealed a predominant localization of the protein to reticular ER-like membranes and the nuclear envelope, consistent with ER localization (Figure 5E). Remarkably, however, in sterol-depleted cells, i.e., under conditions when expression of endogenous TMEM97 is stimulated, a prominent fraction of TMEM97-YFP localized to perinuclear vesicular-like structures and the plasma membrane. Such shift in localization was not observed when sterols were present in the sterol-depleting medium. Coimmunostaining of cells cultivated under these conditions with antibodies recognizing the lysosomal protein Lamp1 showed a significant overlap of the juxtanuclear TMEM97 structures with lysosomal markers (Figure 6A), but not markers of the Golgi complex (data not shown). An overlap of TMEM97-YFP with lysosomal markers was not observed under control culture conditions or in the presence of sterols. However, we cannot exclude the possibility that ER localization of the tagged protein in the presence of sterols might be due to the fact that it is ectopically expressed in cells.

We then quantified the dynamics of TMEM97-YFP localization to lysosomes in response to sterol depletion. Increased perinuclear levels of TMEM97-YFP (Figure 6B, arrows) but not of YFP-tagged ER protein Insig2 or KDEL (Figure 6B, insets) were observed already upon 24 hr culture in LDS, corresponding to ~70% of cholesterol levels of controls (Figures 6B and S1). Notably, localization to lysosomes strongly increased upon further depleting cellular cholesterol levels by adding HPCD, which induced a major fraction of TMEM97-YFP to localize to

Figure 4. Knockdown of the SREBP Target Gene *TMEM97* Reduces LDL Cholesterol Uptake into Endo-/Lysosomal Compartments

(A) Gene expression ($\log_2$) of *TMEM97*, β-actin, and *LDLR* in HeLa cells at 3, 4.5, and 6 hr following cell culture in the absence (−sterols) or presence (+sterols) of sterols (50 μg/ml LDL/10 μg/ml cholesterol) in sterol-depleting culture medium (0.5% LDS/1% HPCD).

(B) Gene expression (fold expression) under control culture conditions upon siRNA knockdown of *LDLR* for 48 hr relative to controls. SiRNA knockdown efficiency was controlled for by western blot against LDLR-GFP (inset).

(C) Gene expression in sterol-depleted HeLa cells upon siRNA knockdown of *SREBP-2*. Inset: graph of the human *TMEM97* gene showing an SRE-1 consensus sequence element 5′ of the transcription initiation site. Expression levels in (A)–(C) were determined by qRT-PCR and normalized to housekeeping gene *RPL19* (n = 3 or 4 experiments/condition) (*$p < 0.05$; **$p < 0.01$; ***$p < 0.001$).

(D) Cellular DiI-LDL (20 min) (images) or Tf568 (15 min) uptake at 37.5°C in HeLa cells transfected with indicated siRNAs, fixed, and counterstained with nuclear dye DRAQ5 and ER-tracker DPX. Endosomal DiI-LDL and Tf568 fluorescence was quantified from automatically acquired background-subtracted images and normalized to nonsilencing controls (*$p < 0.05$; ***$p < 0.001$; n = 4–6 experiments). Bar = 10 μm.

(E) Dynamics of DiI-LDL internalization at 37.5°C into HeLa cells treated with siRNA against *TMEM97* or controls followed over time. Numbers ± SEM of intracellular endosome-like DiI-LDL particles/area (arrows denote examples) were quantified from background-subtracted maximal intensity projections using ImageJ software (n = 4 experiments/time point). Bar = 2 μm.

(F) Analysis of cellular internalization of LDL-associated [^{14}C]cholesterol (20 min; 37.5°C) into HeLa cells upon transfection with indicated siRNAs. Cellular lipids were separated by thin-layer chromatography. Cell-associated free [^{14}C]cholesterol signal (in counts per minute) was quantified by scintillation counting and normalized to controls (*$p < 0.05$; ***$p < 0.001$; n = 5 experiments).

(G) Analysis of total cellular levels of free cholesterol (in μg/mg protein) as determined enzymatically from lipid extracts of HeLa cells transfected with indicated siRNAs (*$p < 0.05$; n = 4 experiments).

(H) HeLa cells transfected with indicated siRNAs stained with Filipin (images) and counterstained for lysosomal protein Lamp1 (data not shown). Filipin signal intensities from automatically acquired background-subtracted images were quantified by DetecTiff (lower panel, analysis mask) and ImageJ (graphs) from either whole cells (left graph, blue) or perinuclear areas (right graph, red) and normalized to controls (n = 6 experiments; ~24 images/condition) (*$p < 0.05$; ***$p < 0.001$). Bar = 10 μm.

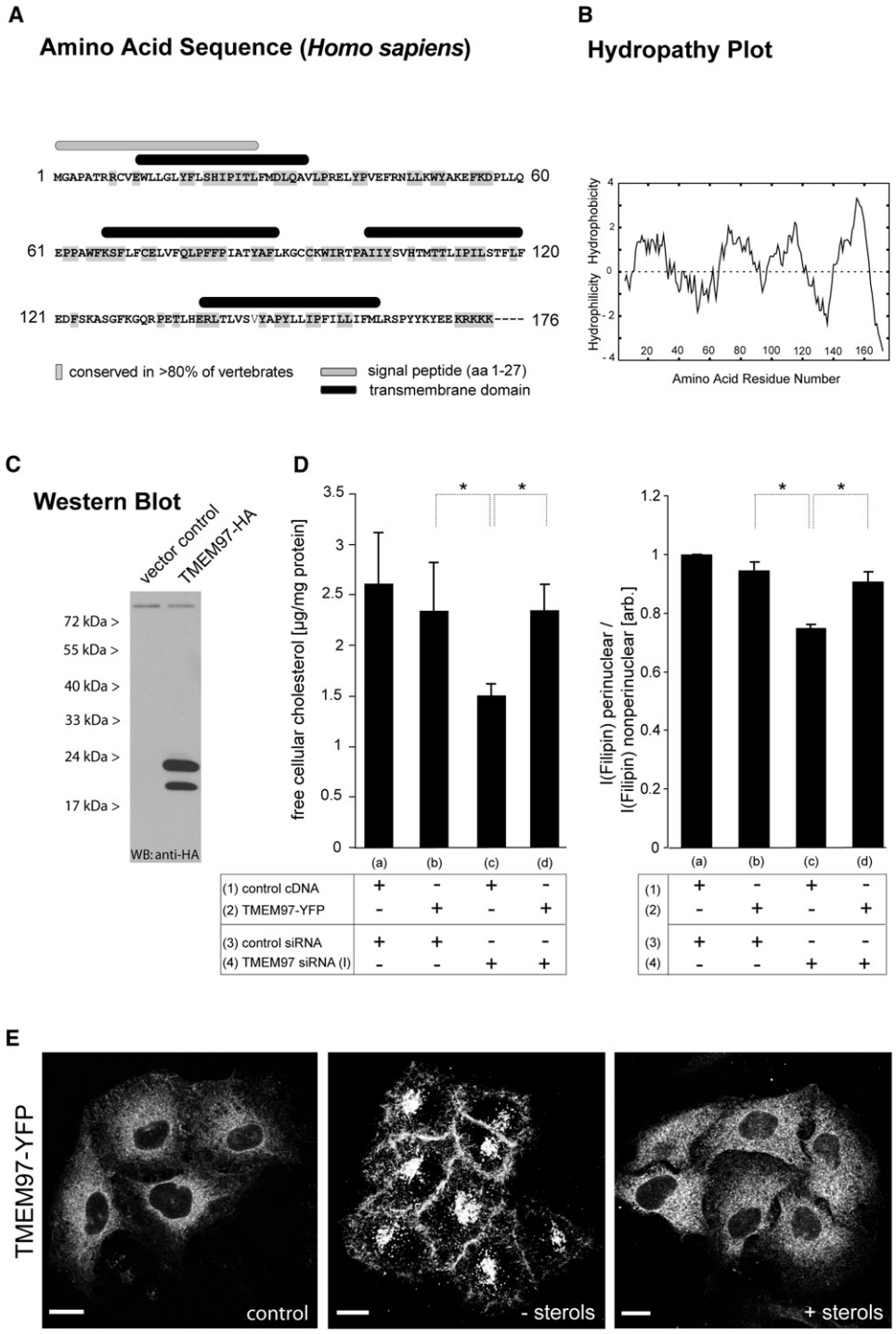

Figure 5. Characterization of Human TMEM97 Protein

(A) Amino acid sequence of full-length human TMEM97 protein. Conserved residues are highlighted. Structural motifs were predicted by ENSEMBL.

(B) Hydropathy blot as calculated by Kyte and Doolittle algorithm using ProtScale.

(C) Western blot analysis of human TMEM97 (linked to 3×HA at the N terminus) in transiently transfected HeLa cells.

(D) Analysis of HeLa cells cotransfected with cDNAs (expressing either TMEM97-YFP [b, d] or a YFP-encoding control plasmid [a, c]) as well as siRNAs (either control siRNA [a, b] or an siRNA targeting the 3′UTR of TMEM97 [c, d]). Forty-eight hours after transfection, lipids were extracted, and total levels of free cellular cholesterol were determined (left graph) (n = 4 experiments; *$p < 0.05$), or cells were stained with Filipin, and signal intensities overlapping with lysosomal marker Lamp1 were quantified by ImageJ (right graph) (n = 3 experiments; ~120 cells/condition; *$p < 0.05$).

(E) Living HeLa cells transiently expressing human TMEM97-YFP cultivated for 48 hr under either control (medium A) or sterol-depleted conditions in the absence (−sterols) (0.5% LDS for 24 hr before adding 1% [w/v] HPCD for 1 hr) or presence (+sterols) (50 µg/ml LDL/10 µg/ml cholesterol) of sterols.

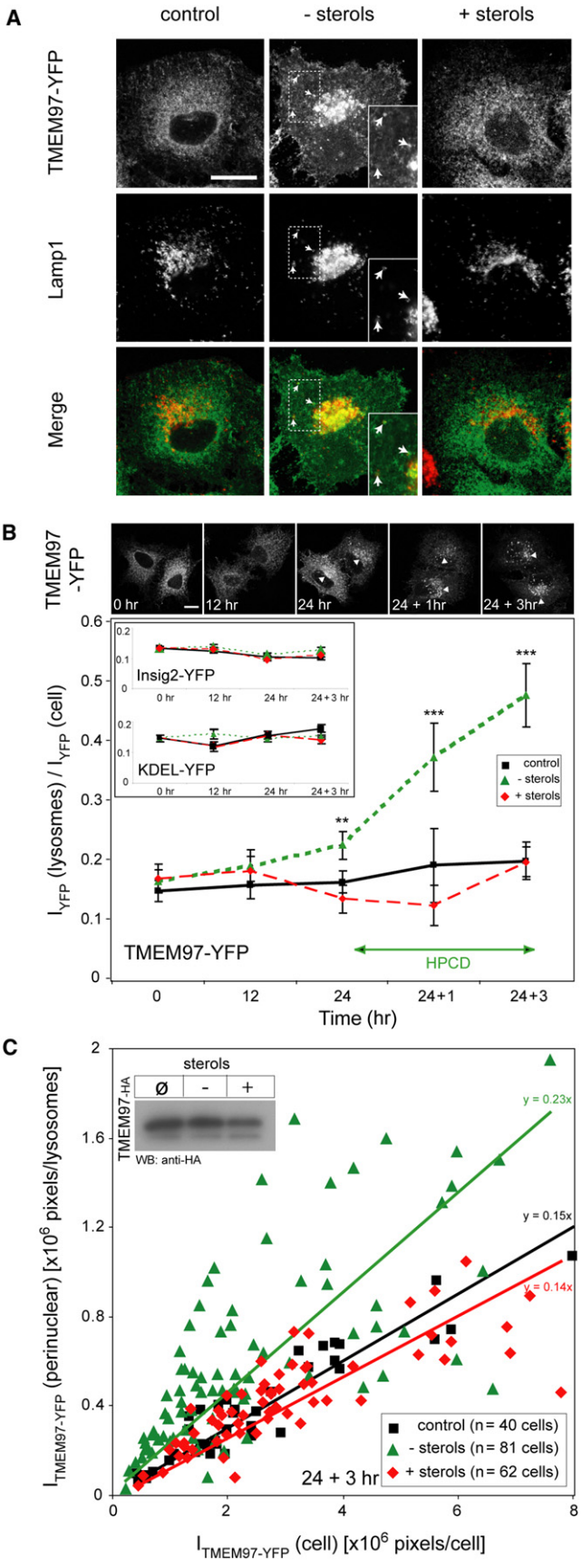

Figure 6. TMEM97 Localizes to Endo-/Lysosomal Compartments in a Sterol-Dependent Manner

(A) HeLa cells expressing human TMEM97-YFP (green) were cultivated under control conditions or in the absence (−sterols) (0.5% LDS for 24 hr before adding 1% [w/v] HPCD for 1 hr) or presence (+sterols) (5% FCS/50 μg/ml LDL/10 μg/ml cholesterol) of sterols. Shown are single slices of confocal stacks from paraformaldehyde-fixed cells expressing TMEM97-YFP counterstained for Lamp1 (red). Arrows denote selected lysosomes.

(B and C) TMEM97-YFP (images), Insig2-YFP, and KDEL-YFP (insets) signal intensities in Lamp1-positive perinuclear compartments (I_{YFP} [lysosomes]; arrows) relative to total cell area (I_{YFP} [cell]) (y axis) in HeLa cells cultivated under control conditions (black) or in the absence (green) or presence (red) of sterols for indicated time points (x axis) as quantified by ImageJ. For sterol depletion, cells were cultivated in 0.5% LDS for up to 24 hr before adding HPCD for 1 hr (24 + 1 hr) resp. 3 hr (24 + 3 hr) (n = 3 experiments; ~50 cells/time point and condition; $^{**}p < 0.01$; $^{***}p < 0.001$). Bars = 10 μm. In (C), intensities of perinuclear relative to total cellular TMEM97-YFP signal are shown at the indicated time point (24 + 3 hr) for a population of individual cells (dots). Formulas indicate linear regression curves. Inset: western blot analysis of TMEM97-3×HA under control culture conditions or in the absence (24 + 3 hr) or presence of sterols.

lysosomes within an interval of only 3 hr (Figure 6B). Lysosomal enrichment was independent of total cellular levels of TMEM97-YFP and not explained by increased abundance of the heterologous protein in sterol-depleted cells (Figure 6C).

Following its internalization into the endo-/lysosomal system, LDL-derived cholesterol is distributed to subsequent cellular compartments by mechanisms that involve NPC1 and NPC2 proteins. Of these, NPC1 is a cholesterol-binding integral membrane protein that is essential for efficient lysosomal cholesterol export (Chang et al., 2006; Ikonen, 2008). Based on our findings of reduced uptake and lysosomal levels of LDL-derived cholesterol in TMEM97 knockdown cells and the localization of TMEM97-YFP to endo-/lysosomal compartments in sterol-depleted cells, we hypothesized that a potential cholesterol regulatory function of TMEM97 in lysosomes could be connected to that of NPC1. Consistent with this, TMEM97-YFP and NPC1 colocalized in vesicular structures of sterol-depleted cells (Figure 7A). In order to test whether the two proteins might physically interact, we performed coimmunoprecipitation experiments. Importantly, an antibody targeting endogenous NPC1 but not a control protein (data not shown) was able to specifically pull down TMEM97 from lysates of TMEM97-expressing HeLa cells (Figure 7B). Coimmunoprecipitation was possible already under control culture conditions, yet it appeared increased in the absence and reduced in the presence of sterols, thereby correlating with the amount of TMEM97 in endo-/lysosomal compartments under these conditions.

In summary, our combined results demonstrate that TMEM97 is an SREBP target gene that under sterol-depleted conditions localizes to lysosomes, directly or indirectly binds to NPC1 protein, and contributes to regulate cellular cholesterol levels at the endo-/lysosomal compartments level.

DISCUSSION

Here, we aimed at identifying genes with functional relevance to cellular cholesterol homeostasis. We assumed that a gene is

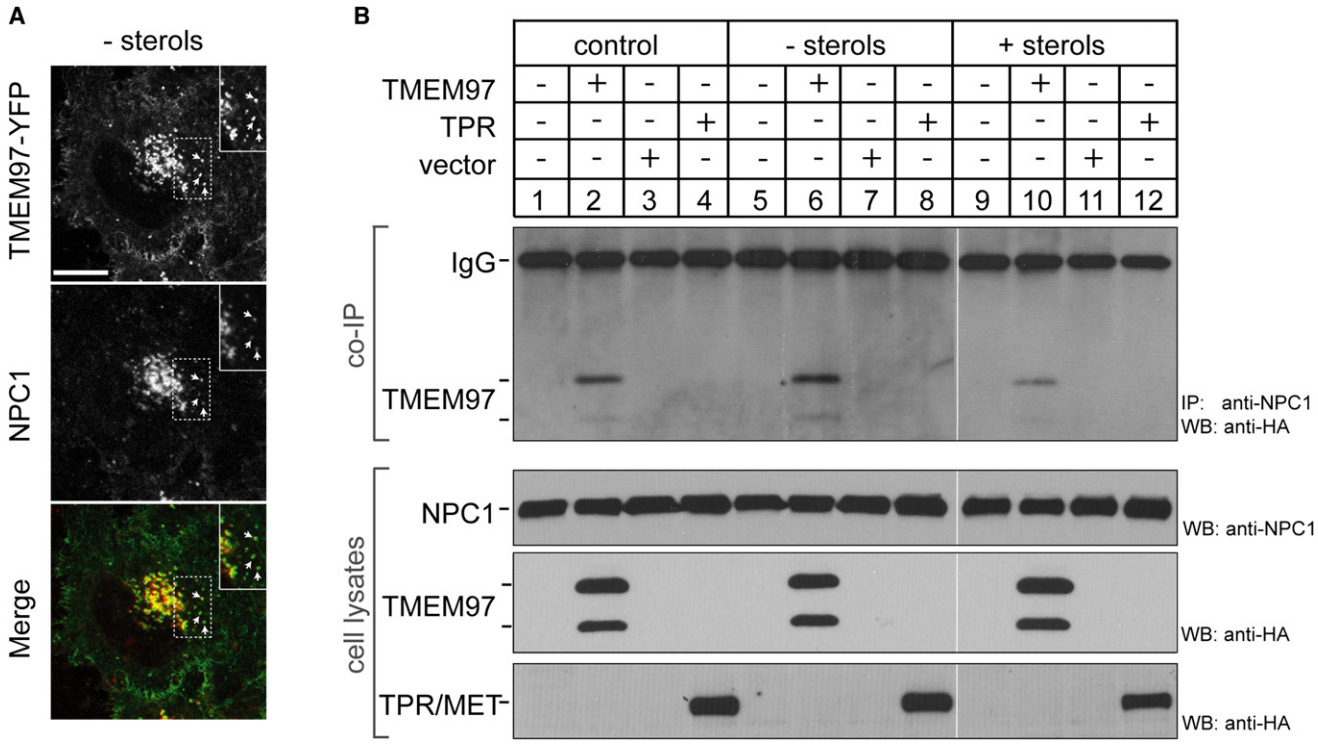

Figure 7. TMEM97 Colocalizes with and Binds to NPC1 Protein

(A) HeLa cells expressing human TMEM97-YFP (green) cultivated under sterol-depleted conditions (0.5% LDS for 24 hr before adding HPCD for 1 hr; 24 + 1 hr; −sterols) were counterstained for endogenous NPC1 (red). Shown are single slices of confocal stacks from paraformaldehyde-fixed cells. Arrows denote selected lysosomes.

(B) Lysates (lower panels) from HeLa cells expressing TMEM97-3×HA, 3×HA-tagged control protein TPR/MET (activated receptor tyrosine kinase MET oncogene) (Schaaf et al., 2005), or HA vector alone under control conditions (lanes 1–4) or in the absence (24 + 1 hr; lanes 5–8) or presence (lanes 9–12) of sterols were subjected to immunoprecipitation (upper panel) with rabbit polyclonal anti-NPC1 antibody. Fractions were immunoblotted with monoclonal anti-HA IgG or anti-NPC1 antibody. Of each sample, ~10% was used for western blotting, while ~90% was used for coimmunoprecipitation.

more likely to be of immediate functional importance if multiple lines of evidence support its role in regulating cellular cholesterol levels. Therefore, several systematic functional genomics strategies were combined. First, candidate genes were identified by genome-wide gene expression analyses of sterol-depleted cultured cells and by systematic literature queries. Then, the function of 100 selected genes was assayed by systematic siRNA knockdown with two cell-based RNAi screens. To minimize the risk of false-positive findings, as they are inherent in large-scale RNAi screens, each gene was probed with six unique siRNAs from two independent siRNA libraries. Moreover, RNAi screening with cell microarrays (Erfle et al., 2007) allowed for high experimental replica numbers, thus further reducing false-positive results. Our integrative approach identified a number of genes that, as demonstrated by silencing with multiple siRNAs, may constitute validated regulators of cellular cholesterol levels and/or Dil-LDL uptake.

Among the validated regulators, we found enrichment for factors with established (*SCAP*) (Nohturfft et al., 2000) or recently described (*LRP6*) (Liu et al., 2008) roles in cellular cholesterol regulation. Mutations in *SCAP* and *LRP6* have been reported as causative for imbalanced blood lipoprotein levels that predispose to cardiovascular disease and myocardial infarction (Mani et al., 2007; Friedlander et al., 2008). Mutations in prosaposin (*PSAP*), knockdown of which increased perinuclear Filipin signals, cause prosaposin deficiency, a lysosomal sphingolipid storage disorder that clinically and in tissues may phenocopy the cholesterol-trafficking disease NPC (Bradová et al., 1993). Reduced function of betaine-homocysteine-methyltransferase 2 (*BHMT2*) decreased cellular Filipin signals as well as Dil-LDL uptake but is also likely to increase homocysteine levels. As hyperhomocysteinemia is well known to directly correlate with increased risk of premature cardiovascular disease (Verhoef et al., 1997), it is tempting to speculate that proatherogenic effects of homocysteine interrelate with impaired lipid metabolism.

For several of the validated regulators, our results confirm and extend previously described molecular functions. E.g., silencing of karyopherin1 (*KPNB1*) strongly reduced cellular Dil-LDL uptake, which is consistent with its role in mediating nuclear translocation of transcriptional active SREBP-2 (Nagoshi et al., 1999). Also, *ID3* is likely to directly affect SREBP-mediated expression regulation by formation of nonfunctional heterodimers with transcriptional active SREBP-1c (Moldes et al., 1999). Reduced levels of ID3 may thus potentiate SREBP transcriptional activation, leading to increased cholesterol levels, as observed in ID3 knockdown cells. Conversely, SREBPs themselves could act as dominant-negative regulators of ID family members, which would explain strongly reduced *ID1*, *ID2*, and

ID3 mRNA levels in our gene expression analysis of sterol-depleted cells and points to a general role of this protein family in regulating cellular lipid metabolism.

Importantly, several of the newly identified regulators have known roles in cellular membrane transport. E.g., synaptophysin (*SYP*) is a cholesterol-binding protein important for biogenesis of synaptic vesicles (Thiele et al., 2000), knockdown of which stimulated DiI-LDL uptake into nonneuronal HeLa cells. Silencing of *AP1S2* not only increased cellular Filipin signal, but was also inhibitory in our parallel RNAi screen studying cellular transferrin uptake. The AP1 complex is crucial for recruiting clathrin to membranes, participates in postendocytic sorting of membrane receptors in polarized cells (among them LDLR and TFRC), and coordinates vesicular transport between endosomes and the Golgi (Gan et al., 2002). Inhibition of AP1S2, like inhibition of other membrane transport regulators (Urano et al., 2008), is therefore not unlikely to affect subcellular cholesterol transport and also recycling of TFRC to the plasma membrane. Interestingly, however, knockdown of AP1S2 had no effect on DiI-LDL uptake, indicating that in HeLa cells the AP1 complex might differentially regulate postendocytic sorting of LDLR and TFRC. Altogether, these results demonstrate that our approach allows convincing identification of candidates with a direct or indirect role in cholesterol homeostasis.

Therefore, although the molecular roles of the 12 other validated candidates identified in our RNAi screens remain elusive, the likelihood that they represent cholesterol regulators is high. Six of these genes were identified based on their pronounced transcriptional activation (*C17orf59*, *ETV5*, *SYTL2*, *TMEM97*, and *VRK3*) or repression (*GBP3*) in response to sterol depletion and have not previously been linked to lipid metabolism. The other six genes were selected from literature and have at most been indirectly related to processes of importance to lipid homeostasis that may involve cellular signaling (*LTBP1* and *NDRG1*), subcellular transport (*C20orf79*, *FDX1*, and *TMSB10*), and intermediary metabolism (*GOT1*).

To independently substantiate our functional genomics strategy with one of the cholesterol regulators identified here, *TMEM97* was chosen to be analyzed in greater detail. One previous study has shown that *TMEM97* (*Mac30*) expression occurs in coordination with genes of cholesterol biosynthesis (Wilcox et al., 2007). Most interestingly, it was also found among a small number of genes whose mRNA levels were increased in livers of mice transgenic for SREBP but decreased in SCAP$-/-$ mice (Horton et al., 2003), suggesting that *TMEM97* might be an SREBP target gene. We show here that, on a cellular level, expression of *TMEM97* is highly sensitive to alterations in sterol levels and propose, consistent with the literature and our own results, that this is regulated via SREBP and a sterol-response element upstream of the human *TMEM97* gene. Our siRNA knockdown experiments demonstrate loss of TMEM97 function as inhibitory for both cellular levels as well as internalization of cholesterol from LDL. Importantly, cholesterol levels in TMEM97-deficient cells were most profoundly reduced in compartments overlapping with endo-/lysosomal markers. Lysosomal cholesterol is of special relevance to cellular cholesterol homeostasis, as from this compartment LDL-derived cholesterol is transferred to the ER where it exerts regulatory functions (Pentchev et al., 1987; Infante et al., 2008). How cholesterol transport between these compartments is achieved has not yet been fully clarified. NPC1 and NPC2 proteins are central regulators in this process, as malfunction of these factors may cause massive accumulation of cholesterol in the endo-/lysosomal system, as seen in NPC disease (Chang et al., 2006; Ikonen, 2008). The observation that in sterol-depleted cells TMEM97-YFP localizes to the endo-/lysosomal system and the plasma membrane suggests that endogenous TMEM97 might exert its cholesterol regulatory function in these compartments. Our finding that TMEM97 colocalizes and directly or indirectly interacts with NPC1 implies that, rather than being involved in the immediate endocytic uptake of LDL, TMEM97 contributes to regulate LDL-cholesterol trafficking toward or away from lysosomes. In NPC1-deficient cells, lysosomal cholesterol as well as LDL uptake is increased (Pentchev et al., 1987), while both these processes were reduced in TMEM97 knockdown cells. Thus, one hypothesis of how TMEM97 and NPC1 could functionally interact is that upon stimulation of *TMEM97* expression by activated SREBP, TMEM97 is transported to lysosomes, where it might induce NPC1 to modify its cholesterol transport activity. Detailed analyses of the mechanisms by which TMEM97 is enriched in endo-/lysosomal compartments of sterol-depleted cells and how this may affect cholesterol regulatory events in lysosomes and functionally related compartments await to be clarified in further studies.

Taken together, our approach has uncovered a number of genes with a high likelihood of being immediately functionally relevant to cellular cholesterol regulation and potentially also disease. Disease-associated genes affecting plasma cholesterol levels have successfully been identified in single families and, more recently, large-scale linkage and association studies (Manolio, 2009). Conversely, using cultured cell models in combination with genetic complementation has proven successful to delineate most of the machinery that keep cellular cholesterol levels balanced (Goldstein et al., 2002). Integrated functional genomics, as applied here, now harbors significant potential not only to ease identification, but also to allow functional characterization of regulators of cholesterol homeostasis in health and disease.

EXPERIMENTAL PROCEDURES

Antibodies and Materials

Mouse monoclonal antibodies against LAMP1 and HA were from DSHB (University of Iowa) and Sigma, respectively. Rabbit polyclonal antibody against NPC1 was from Novus Biologicals (Littleton, CO). For further materials, expression of markers, and coimmunoprecipitation conditions, see Supplemental Data.

Sterol Depletion

For sterol depletion, cells cultivated in DMEM/2 mM L-glutamine/100 IU/ml penicillin/100 mg/ml streptomycin/0.5% LDS for up to 24 hr were exposed to 2% (w/v) HPCD for 3 hr (for expression profiling) or 1% HPCD for indicated time points (for further experiments) (Runz et al., 2006). Where indicated, sterol depletion was counteracted by simultaneously adding 50 μg/ml LDL/10 μg/ml cholesterol. For details on cell culture and how cellular sterols were modified and analyzed, see Supplemental Data.

RNA Isolation and Gene Expression Analysis

For expression profiling using human RZPD3 cDNA microarrays (Wagner et al., 2004) and qRT-PCR, see Supplemental Data.

Design and Production of Transfected siRNA Microarrays

One hundred candidate genes were selected for RNAi screening (Table S3): 64 genes, typically not previously linked to cellular cholesterol regulation, were chosen based on transcriptional response to sterol depletion. Of these, 28 genes were from gene expression group I or X (strongest transcriptional activation and repression upon sterol depletion, respectively), 17 genes from group II or IX, and 19 genes from groups III–VIII. Additionally, 36 genes were chosen from a list of ~600 genes that had been generated by systematic PubMed queries using the respective NCBI Gene Symbol in combination with the keywords cholesterol, atherosclerosis, or lipid (see Table S3 and Supplemental Data for source articles). For RNAi screening, two custom siRNA microarrays consisting of 308 siRNA transfection mixes/array were designed and produced as described (Erfle et al., 2007). Each of the 100 genes was represented by 6 distinct, chemically synthesized 21 nt siRNAs from either QIAGEN (siRNA library I) or Ambion/Applied Biosystems (siRNA library II) (Tables S4 and S5). Previously validated siRNAs against five genes were selected as controls: *INCENP*, inducing multinucleated arrested cells that served to monitor siRNA transfection efficiency (Neumann et al., 2006); *LDLR*, reducing DiI-LDL uptake to ~25% and perinuclear Filipin signal to ~60%; *NPC2*, increasing perinuclear Filipin signal to ~150%; *COPB1*, reducing DiI-LDL uptake to ~5%; and *TFRC*, reducing Tf568 uptake to ~50% (Tables S4 and S5). Scrambled siRNA (randomized siRNA sequence not targeting any human gene) (Neumann et al., 2006) and Ambion negative control siRNA-1 (Neg-1) were represented on nine spots of the respective array.

Functional RNAi Screening Assays

HeLa cells were plated on cell microarrays at a density of 1×10^5 cells and cultivated and reverse siRNA-transfected as described (Erfle et al., 2007). For Filipin assay (Runz et al., 2006), culture conditions were maintained until 48 hr after seeding cells were fixed with 3% paraformaldehyde, stained with 50 μg/ml Filipin in PBS from a stock solution of 1 mg/ml in dimethylformamide, and counterstained for Lamp1 and nuclear marker DRAQ5 (Biostatus Limited; Leicestershire, UK). For DiI-LDL uptake assay (Gilbert et al., 2009), medium was exchanged 32 hr after seeding for DMEM/2 mM L-glutamine/100 IU/ml penicillin/100 μg/ml streptomycin/0.2% (w/v) BSA, and cells were cultivated for another 15 hr before adding 1% HPCD for 45 min. Cells were washed with ice-cold imaging solution (MEM without phenol red, containing 30 mM HEPES and 0.5 g/l $NaHCO_3$ [pH 7.4]) (Invitrogen)/0.2% BSA and labeled with 50 μg/ml DiI-LDL (Invitrogen) for 30 min at 4°C. DiI-LDL uptake was stimulated for 20 min at 37.5°C. Cells were then washed for 1 min in imaging solution (pH 3.5) at 4°C, fixed, and counterstained for nuclei and ER (ER-Tracker DPX, Invitrogen). For Tf568 uptake assay, 47 hr after seeding, medium was exchanged for imaging solution/0.2% BSA for 60 min. Cells were washed and labeled at 4°C with 60 μg/ml Tf568 (Invitrogen) in imaging solution/0.2% BSA. After 30 min, medium was exchanged for imaging solution/0.2% (w/v) BSA/300 μg/ml apo-transferrin (Invitrogen) and incubated for 15 min at 37.5°C before fixation and counterstaining for nuclei and ER.

Image Acquisition and Data Analysis

Images were acquired as described (Simpson et al., 2007) and quantitatively analyzed using the software DetecTiff (Gilbert et al., 2009) or NIH ImageJ (Wayne Rasband Analytics, NIH; Bethesda, MD). For details, see Supplemental Data.

ACCESSION NUMBERS

The complete microarray data are available online at the public microarray database ArrayExpress (accession number E-TABM-599).

SUPPLEMENTAL DATA

Supplemental Data include Supplemental Experimental Procedures, Supplemental References, seven figures, seven tables, and one movie and can be found online at http://www.cell.com/cell-metabolism/supplemental/S1550-4131(09)00157-0.

ACKNOWLEDGMENTS

We are grateful to B. Neumann, C. Conrad, and J. Bulkescher for support in image acquisition and helpful discussions, N. Beil for preparing cell microarrays, O. Oppermann for help with data display, and B. Karten for critical comments on the manuscript. Olympus Biosystems is acknowledged for continuous support of the ALMF at EMBL. The authors declare no conflicts of interest. The work was supported by the Landesstiftung Baden-Württemberg to H.R. (Elite-Postdoc Fellowship) and R.P. (RNS/RNAi) and the Ara Parseghian Medical Research Foundation (APMRF) to H.R.

Received: December 9, 2008
Revised: April 7, 2009
Accepted: May 26, 2009
Published: July 7, 2009

REFERENCES

Börnig, H., and Geyer, G. (1974). Staining of cholesterol with the fluorescent antibiotic "filipin". Acta Histochem. *50*, 110–115.

Bradová, V., Smíd, F., Ulrich-Bott, B., Roggendorf, W., Paton, B.C., and Harzer, K. (1993). Prosaposin deficiency: multiple glycolipid elevations, partial enzyme deficiencies and ultrastructure of the skin in this generalized sphingolipid storage disease. Hum. Genet. *92*, 143–152.

Brown, M.S., and Goldstein, J.L. (1974). Familial hypercholesterolemia: defective binding of lipoproteins to cultured fibroblasts associated with impaired regulation of 3-hydroxy-3-methylglutaryl coenzyme A reductase activity. Proc. Natl. Acad. Sci. USA *71*, 788–792.

Chang, T.Y., Chang, C.C., Ohgamie, N., and Yamauchi, Y. (2006). Cholesterol sensing, trafficking, and esterification. Annu. Rev. Cell Dev. Biol. *22*, 129–157.

Erfle, H., Neumann, B., Liebel, U., Rogers, P., Held, M., Walter, T., Ellenberg, J., and Pepperkok, R. (2007). Reverse transfection on cell arrays for high content screening microscopy. Nat. Protocols *2*, 392–399.

Friedlander, Y., Schwartz, S.M., Durst, R., Meiner, V., Robertson, A.S., Erez, G., Leitersdorf, E., and Siscovick, D.S. (2008). SREBP-2 and SCAP isoforms and risk of early onset myocardial infarction. Atherosclerosis *196*, 896–904.

Gan, Y., McGraw, T.E., and Rodriguez-Boulan, E. (2002). The epithelial-specific adaptor AP1B mediates post-endocytic recycling to the basolateral membrane. Nat. Cell Biol. *4*, 605–609.

Ghosh, R.N., Gelman, D.L., and Maxfield, F.R. (1994). Quantification of low density lipoprotein and transferrin endocytic sorting HEp2 cells using confocal microscopy. J. Cell Sci. *107*, 2177–2189.

Gilbert, D.F., Meinhof, T., Pepperkok, R., and Runz, H. (2009). DetecTiff: A novel image analysis routine for high content screening microscopy. J. Biomol. Screen., in press.

Goldstein, J.L., Rawson, R.B., and Brown, M.S. (2002). Mutant mammalian cells as tools to delineate the sterol regulatory element-binding protein pathway for feedback regulation of lipid synthesis. Arch. Biochem. Biophys. *397*, 139–148.

Goldstein, J.L., DeBose-Boyd, R.A., and Brown, M.S. (2006). Protein sensors for membrane sterols. Cell *124*, 35–46.

Harding, C., Heuser, J., and Stahl, P. (1983). Receptor-mediated endocytosis of transferrin and recycling of the transferrin receptor in rat reticulocytes. J. Cell Biol. *97*, 329–339.

Horton, J.D., Shah, N.A., Warrington, J.A., Anderson, N.N., Park, S.W., Brown, M.S., and Goldstein, J.L. (2003). Combined analysis of oligonucleotide microarray data from transgenic and knockout mice identifies direct SREBP target genes. Proc. Natl. Acad. Sci. USA *100*, 12027–12032.

Ikonen, E. (2008). Cellular cholesterol trafficking and compartmentalization. Nat. Rev. Mol. Cell Biol. *9*, 125–138.

Infante, R.E., Wang, M.L., Radhakrishnan, A., Kwon, H.J., Brown, M.S., and Goldstein, J.L. (2008). NPC2 facilitates bidirectional transfer of cholesterol between NPC1 and lipid bilayers, a step in cholesterol egress from lysosomes. Proc. Natl. Acad. Sci. USA *105*, 15287–15292.

Liebel, U., Starkuviene, V., Erfle, H., Simpson, J.C., Poustka, A., Wiemann, S., and Pepperkok, R. (2003). A microscope-based screening platform for large-scale functional protein analysis in intact cells. FEBS Lett. *554*, 394–398.

Liu, W., Mani, S., Davis, N.R., Sarrafzadegan, N., Kavathas, P.B., and Mani, A. (2008). Mutation in EGFP domain of LDL receptor-related protein 6 impairs cellular LDL clearance. Circ. Res. *103*, 1280–1288.

Mani, A., Radhakrishnan, J., Wang, H., Mani, A., Mani, M.A., Nelson-Williams, C., Carew, K.S., Mane, S., Najmabadi, H., Wu, D., and Lifton, R.P. (2007). LRP6 mutation in a family with early coronary disease and metabolic risk factors. Science *315*, 1278–1282.

Manolio, T.A. (2009). Cohort studies and the genetics of complex disease. Nat. Genet. *41*, 5–6.

Maxfield, F.R., and Tabas, I. (2005). Role of cholesterol and lipid organization in disease. Nature *438*, 612–621.

Moldes, M., Boizard, M., Liepvre, X.L., Feve, B., Dugail, I., and Pairault, J. (1999). Functional antagonism between inhibitor of DNA binding (Id) and adipocyte determination and differentiation factor 1/sterol regulatory element-binding protein-1c (ADD1/SREBP-1c) trans-factors for the regulation of fatty acid synthase promoter in adipocytes. Biochem. J. *344*, 873–880.

Nagoshi, E., Imamoto, N., Sato, R., and Yoneda, Y. (1999). Nuclear import of sterol regulatory element-binding protein-2, a basic helix-loop-helix-leucine zipper (bHLH-Zip)-containing transcription factor, occurs through the direct interaction of importin beta with HLH-Zip. Mol. Biol. Cell *10*, 2221–2233.

Naureckiene, S., Sleat, D.E., Lackland, H., Fensom, A., Vanier, M.T., Wattiaux, R., Jadot, M., and Lobel, P. (2000). Identification of HE1 as the second gene of Niemann-Pick C disease. Science *290*, 2298–2301.

Neumann, B., Held, M., Liebel, U., Erfle, H., Rogers, P., Pepperkok, R., and Ellenberg, J. (2006). High-throughput RNAi screening by time-lapse imaging of live human cells. Nat. Methods *3*, 385–390.

Nohturfft, A., Yabe, D., Goldstein, J.L., Brown, M.S., and Espenshade, P.J. (2000). Regulated step in cholesterol feedback localized to budding of SCAP from ER membranes. Cell *102*, 315–323.

Pentchev, P.G., Comly, M.E., Kruth, H.S., Tokoro, T., Butler, J., Sokol, J., Filling-Katz, M., Quirk, J.M., Marshall, D.C., Patel, S., et al. (1987). Group C Niemann-Pick disease: faulty regulation of low-density lipoprotein uptake and cholesterol storage in cultured fibroblasts. FASEB J. *1*, 40–45.

Runz, H., Miura, K., Weiss, M., and Pepperkok, R. (2006). Sterols regulate ER-export dynamics of secretory cargo protein ts-O45-G. EMBO J. *25*, 2953–2965.

Schaaf, C.P., Benzing, J., Schmitt, T., Erz, D.H., Tewes, M., Bartram, C.R., and Janssen, J.W. (2005). Novel interaction partners of the TPR/MET tyrosine kinase. FASEB J. *19*, 267–269.

Simpson, J.C., Cetin, C., Erfle, H., Joggerst, B., Liebel, U., Ellenberg, J., and Pepperkok, R. (2007). An RNAi screening platform to identify secretion machinery in mammalian cells. J. Biotechnol. *129*, 352–365.

Smith, J.R., Osborne, T.F., Goldstein, J.L., and Brown, M.S. (1990). Identification of nucleotides responsible for enhancer activity of sterol regulatory element in low density lipoprotein receptor gene. J. Biol. Chem. *265*, 2306–2310.

Thiele, C., Hannah, M.J., Fahrenholz, F., and Huttner, W.B. (2000). Cholesterol binds to synaptophysin and is required for biogenesis of synaptic vesicles. Nat. Cell Biol. *2*, 42–49.

Urano, Y., Watanabe, H., Murphy, S.R., Shibuya, Y., Geng, Y., Peden, A.A., Chang, C.C., and Chang, T.Y. (2008). Transport of LDL-derived cholesterol from the NPC1 compartment to the ER involves the trans-Golgi network and the SNARE protein complex. Proc. Natl. Acad. Sci. USA *105*, 16513–16518.

Verhoef, P., Kok, F.J., Kruyssen, D.A., Schouten, E.G., Witteman, J.C., Grobbee, D.E., Ueland, P.M., and Refsum, H. (1997). Plasma total homocysteine, B vitamins, and risk of coronary atherosclerosis. Arterioscler. Thromb. Vasc. Biol. *17*, 989–995.

Wagner, W., Ansorge, A., Wirkner, U., Eckstein, V., Schwager, C., Blake, J., Miesala, K., Selig, J., Saffrich, R., Ansorge, W., and Ho, A.D. (2004). Molecular evidence for stem cell function of the slow-dividing fraction among human hematopoietic progenitor cells by genome-wide analysis. Blood *104*, 675–686.

Whitney, J.A., Gomez, M., Sheff, D., Kreis, T.E., and Mellman, I. (1995). Cytoplasmic coat proteins involved in endosome function. Cell *83*, 703–713.

Wilcox, C.B., Feddes, G.O., Willett-Brozick, J.E., Hsu, L.C., DeLoia, J.A., and Baysal, B.E. (2007). Coordinate up-regulation of TMEM97 and cholesterol biosynthesis genes in normal ovarian surface epithelial cells treated with progesterone: implications for pathogenesis of ovarian cancer. BMC Cancer *7*, 223.